*Journal of Applied Electrochemistry* **34**: 1177–1184, 2004.



# Application of a Doehlert experimental design to the optimization of an Au–Co plating electrolyte

L. CHALUMEAU[1], M. WERY[1]*, H.F. AYEDI[2], M.M. CHABOUNI[3] and C. LECLERE[4]
[1]*Laboratoire de Chimie des Matériaux et des Interfaces, Université de Franche, Comté-Route de Gray, 25030 Besançon, France*
[2]*URCI, Ecole Nationale d'Ingénieurs de Sfax-BP, W-3038 Sfax, Tunisie*
[3]*LCI, Ecole Nationale d'Ingénieurs de Sfax-BP, W-3038 Sfax, Tunisie*
[4]*Métalor SA, DAT-R&D, 41 Rue de Paris, 93130 Noisy le Sec, France*
*(*author for correspondence, e-mail: martine.wery@univ.fcomte.fr)*

Received 6 November 2003; accepted in revised form 7 July 2004

*Key words:* canonical analysis, Doehlert experimental design, GDOES, gold electrodeposit, XPS

**Abstract**

Electrodeposited cobalt hardened gold is widely used for electronic applications. The aim of this study was to investigate and optimize the performances of the plating electrolyte (cathodic efficiency and deposition rate) and the composition of the Au–Co coating. A four variable Doehlert experimental design was applied to this optimization and validation was carried out by means of statistical analysis. In a second step, the 'optimal' Au–Co electrodeposit was examined by spectroscopy techniques (GDOES, XPS).

## 1. Introduction

Hard gold electrodeposits have been widely used as a contact material in various electronic terminal devices due to their unique feature combining physical and electrical properties [1–3]. So-called 'hard gold' is, in fact, an alloy containing a small percentage of a hardening metal – usually nickel or cobalt (from 0.3 to 1.6 atom percent (a/o) i.e. 0.1–0.5 weight percent (w/o)) [1–21] – although use of other metals [22–24] and additive-free gold [25–28] have also been reported. Over the past few years, there has been increasing interest in cobalt as an alloying partner to replace allergenic nickel. A small cobalt addition in buffered acid solutions of $KAu(CN)_2$ raises the hardness of the plated layer to 140–220 Hv and yields surfaces having low and stable contact resistance (3–7 m$\Omega$) as well as good wear resistance. So, the commercial and economic importance of cobalt-hardened gold has led to extensive investigations into (i) the properties and microstructure of the deposits [16–21] (ii) the chemical state of cobalt in cobalt-hardened gold coatings [16–19, 29–32] (iii) the incorporation of foreign elements such as carbon, nitrogen and potassium in the deposits [29–35].

The aim of the present study was to investigate the combined effect of the Au–Co electrolyte composition and the current density on both the performances of the plating solution (deposition rate, cathodic efficiency) and the cobalt content in the electrodeposit. Previous studies on performances of Au–Co electrolytes and properties of electrodeposits have investigated the influence of each parameter one at a time while keeping the others constant. We have viewed the problem from a different angle. Because parameters in a plating operation are numerous and co-exist in complex relationships, the application of an experimental design such a Doehlert design [36] seems the most suitable experimental approach to optimize the performances of the electrolyte and the composition of the Au–Co deposit via the composition of the plating solution. The first step was to determine the optimum composition of the plating solution, which led to maximize the cathodic efficiency and the deposition rate and to limit the cobalt content of the coating. Next, the characteristics of the Au–Co electrodeposit corresponding to the optimum composition were investigated using spectroscopy techniques (GDOES, XPS).

## 2. Experimental techniques

### 2.1. *Samples*

All hard gold films were plated in a proprietary bath (commercially known as Engold 2010 CHS purchased from Metalor SA). The bath was composed of a potassium gold cyanide salt, a citric acid as the buffer, a cobalt salt as the hardening-brightening agent and a

pyridinic brightener. Plating was carried out at 55 °C. All gold coatings were deposited onto nickel-plated brass disk (0.5 mm thick–20 mm diameter) using a rotating disk cathode (1000 rpm) to provide a well-defined geometry and agitation. Other parameters were adjusted in accordance with each process technical data sheet i.e. gold, cobalt and brightener concentrations and pH.

### 2.2. *Measurement procedures*

- *Cobalt conten*t: The cobalt content was measured by atomic absorption spectroscopy.
- *Cathodic efficiency*: The cathodic efficiency for gold deposition was determined by weighing the nickel-plated disk before and after plating.
- *Glow discharge optical emission spectroscopy (GDOES)*.

The distribution of impurity species in the gold layers was determined by depth profiling using a LECO GDOES 750 A instrument. 700 V and 20 mA were chosen as measurement parameters for the excitation and sputtering process. The analysis area was 4 mm in diameter. The sputtering layer was 0.1 $\mu$m thick. The following atomic emission lines were: C: 156.143 nm, Co: 345.351 nm, N: 174.724 nm, K: 766.490 nm, Au: 242.795 nm, Ni: 341.477 nm and Cu: 327.396 nm.

- *X-ray photoelectron spectroscopy (XPS)*.

An S-Probe (SSI) equipped with a hemispherical analyser was used. AlK$\alpha$ radiation of 1486.7 eV energy was applied for excitation. The vacuum conditions for the analyser chamber were nearly $10^{-10}$ mbar during analysis. The analysed area was about $300\times1200$ $\mu m^2$.

### 2.3. *Doehlert experimental design*

The Doehlert experimental design [36] was used to study the effect of the plating conditions on the performances of the plating bath and the coating properties. Among the Doehlert design properties, one involved uniform distribution: a set of points was uniformly distributed in space, thus allowing exploration of the whole experimental domain. The variables $U_j$ selected were:

$U_1$: Gold concentration in the plating bath (g $l^{-1}$).
$U_2$: pH of the plating bath.
$U_3$: Current density (A $dm^{-2}$).
$U_4$: Cobalt concentration in the plating bath (g $l^{-1}$).

To simplify the calculations, coded variables $X_j$ were used instead of natural variables $U_j$ [36].

For the Doehlert design construction, its centre and variation step as shown in Table 1 defined the study domain.

Three responses were studied: $Y_1$: cathodic efficiency (% wt), $Y_2$: deposition rate (mg $min^{-1}$) and $Y_3$: cobalt content in the gold–cobalt coating (ppm).

A full quadratic model with 15 coefficients, including interaction terms, was assumed to describe relationship between each response $Y_i$ and experimental factors $X_j$:

*Table 1.* Experimental domain

| Variables | Levels | Centre $U_j(0)$ | Step $\Delta U_j$ |
|---|---|---|---|
| $U_1$ (g $l^{-1}$) | 5 | 8.5 | 6.5 |
| $U_2$ (u pH) | 7 | 4.5 | 0.5 |
| $U_3$ (A $dm^{-2}$) | 7 | 15 | 10 |
| $U_4$ (g $l^{-1}$) | 3 | 1.0 | 0.5 |

$$\hat{Y} = b_0 + \sum_{j=1}^{j=4} b_j X_j + \sum_{j=1}^{j=3}\sum_{k=2}^{k=4} b_{jk} X_j X_k + \sum_{j=1}^{j=4} b_{jj} X_j^2$$

where $b_0$ is the constant of the model; $b_j$, the first degree coefficients; $b_{jk}$, the cross-product coefficients and $b_{jj}$, the quadratic coefficients.

The Doehlert matrix required attribution of different levels to the selected variables. If the number of factors is $k$, then in addition to the centre point, a total of $k^2 + k$ design points lie on hypersphere of radius one. So, the total assay number ($N = k^2 + k + 1$) is generally low: with four factors this number is 21.

In this work, we used Nemrod W software [37] for data calculation and treatment.

## 3. Results and discussion

### 3.1. *Response models and validation*

Table 2 shows the Doehlert experimental design in coded variables and the obtained responses $Y_i$. Fitted to 21 responses values (Table 2), the second order models are represented by the following equations:

*Table 2.* Experimental design (coded) and responses values

| No. of exp. | Factors | | | | Responses | | |
|---|---|---|---|---|---|---|---|
| | $X_1$ | $X_2$ | $X_3$ | $X_4$ | $Y_1$ | $Y_2$ | $Y_3$ |
| 1 | 1.0000 | 0.0000 | 0.0000 | 0.0000 | 25.26 | 66.2 | 1434 |
| 2 | −1.0000 | 0.0000 | 0.0000 | 0.0000 | 7.71 | 20.2 | 4285 |
| 3 | 0.5000 | 0.8660 | 0.0000 | 0.0000 | 32.66 | 85.6 | 986 |
| 4 | −0.5000 | −0.8660 | 0.0000 | 0.0000 | 10.91 | 28.6 | 2813 |
| 5 | 0.5000 | −0.8660 | 0.0000 | 0.0000 | 18.77 | 49.2 | 2156 |
| 6 | −0.5000 | 0.8660 | 0.0000 | 0.0000 | 16.02 | 42.0 | 1981 |
| 7 | 0.5000 | 0.2887 | 0.8165 | 0.0000 | 20.63 | 83.6 | 1281 |
| 8 | −0.5000 | −0.2887 | −0.8165 | 0.0000 | 33.59 | 40.2 | 2020 |
| 9 | 0.5000 | −0.2887 | −0.8165 | 0.0000 | 49.63 | 59.4 | 1728 |
| 10 | 0.0000 | 0.5774 | −0.8165 | 0.0000 | 50.63 | 60.6 | 1304 |
| 11 | −0.5000 | 0.2887 | 0.8165 | 0.0000 | 9.62 | 39.0 | 2542 |
| 12 | 0.0000 | −0.5774 | 0.8165 | 0.0000 | 13.47 | 54.6 | 2304 |
| 13 | 0.5000 | 0.2887 | 0.2041 | 0.7906 | 40.85 | 121.8 | 2179 |
| 14 | −0.5000 | −0.2887 | −0.2041 | −0.7906 | 18.87 | 42.8 | 2576 |
| 15 | 0.5000 | −0.2887 | −0.2041 | −0.7906 | 43.13 | 97.8 | 1551 |
| 16 | 0.0000 | 0.5774 | −0.2041 | −0.7906 | 38.98 | 88.4 | 1641 |
| 17 | 0.0000 | 0.0000 | 0.6124 | −0.7906 | 23.87 | 88.2 | 1158 |
| 18 | −0.5000 | 0.2887 | 0.2041 | 0.7906 | 24.15 | 72.0 | 4118 |
| 19 | 0.0000 | −0.5774 | 0.2041 | 0.7906 | 19.65 | 58.6 | 3016 |
| 20 | 0.0000 | 0.0000 | −0.6124 | 0.7906 | 39.64 | 61.6 | 2481 |
| 21 | 0.0000 | 0.0000 | 0.0000 | 0.0000 | 22.58 | 59.2 | 1520 |

*Table 3.* ANOVA table for the responses $\hat{Y}_1$, $\hat{Y}_2$ and $\hat{Y}_3$

| Response | Source | Sum of squares | Degrees of freedom (df) | Mean square | $F$ | Significance |
|---|---|---|---|---|---|---|
| $\hat{Y}_1$ | Regression | $3.25649 \times 10^3$ | 14 | $2.32606 \times 10^2$ | 9.4038 | 0.685** |
| | Residual | $1.48413 \times 10^2$ | 6 | $2.47355 \times 10^1$ | | |
| | Total | $3.40490 \times 10^3$ | 20 | | | |
| $\hat{Y}_2$ | Regression | $1.11150 \times 10^4$ | 14 | $7.93935 \times 10^2$ | 4.1972 | 4.47* |
| | Residual | $1.13496 \times 10^3$ | 6 | $1.89160 \times 10^2$ | | |
| | Total | $1.22500 \times 10^4$ | 20 | | | |
| $\hat{Y}_3$ | Regression | $1.49445 \times 10^7$ | 14 | $1.06747 \times 10^6$ | 9.0706 | 0.745** |
| | Residual | $7.06101 \times 10^5$ | 6 | $1.17683 \times 10^5$ | | |
| | Total | $1.56506 \times 10^7$ | 20 | | | |

The significance in the table is the probability (between 0 and 1) of obtaining a ratio of mean squares greater than $F$. The significance level is represented in the conventional manner: ** < 0.01 (1%) and * < 0.05 (5%) [38].

$$\hat{Y}_1 = 22.58 + 12.76X_1 + 6.93X_2 - 17.32X_3 - 0.09X_4 + 5.07X_1X_2 - 4.87X_1X_3 - 3.74X_2X_3 - 5.37X_1X_4 + 6.03X_2X_4 + 7.29X_3X_4 - 6.10X_1^2 - 1.96X_2^2 + 12.54X_3^2 + 12.80X_4^2$$

$$\hat{Y}_2 = 59.2 + 32.5X_1 + 17.2X_2 + 7.0X_3 - 0.5X_4 + 13.3X_1X_2 + 10.9X_1X_3 + 0.9X_2X_3 - 10.9X_1X_4 + 18.5X_2X_4 + 14.2X_3X_4 - 16.0X_1^2 - 5.1X_2^2 + 0.8X_3^2 + 35.6X_4^2$$

$$\hat{Y}_3 = 1520 - 1187X_1 - 491X_2 + 158X_3 + 770X_4 - 195X_1X_2 - 524X_1X_3 - 287X_2X_3 - 371X_1X_4 + 53X_2X_4 + 756X_3X_4 + 1340X_1^2 + 172X_2^2 + 137X_3^2 + 982X_4^2$$

Table 3 shows the analysis of variance (ANOVA) for the three responses. As it can be seen, the regression sum of squares is statistically significant (their $p$ value is less than 0.05) [38–41]. The residual sum of squares is calculated with 6 degrees of freedom (df) for testing the adequacy of the fitted model. For the responses $\hat{Y}_1$, $\hat{Y}_2$ and $\hat{Y}_3$, the multiple correlation coefficients are respectively 0.956, 0.907 and 0.955. These values indicate how well the derivate models fitted the experimental data. We can then conclude that each second order model is adequate and can be used as prediction equation.

### 3.2. *Canonical analysis*

The purpose of the following paragraph is to find out the best experimental conditions, which lead to maximize the cathodic efficiency ($Y_1$) and the deposition rate ($Y_2$) and to limit the cobalt content of the coating ($Y_3$) in the range 2000–3000 ppm.

The second order model with square terms describes a variety of shaped response surfaces. The stationary point of the response surface can be a maximum, a minimum or a saddle point (minimax). It is rather difficult to comprehend how the surface is shaped by mere inspection of the algebraic expression of the model. But the nature of the stationary point is conveniently determined by a canonical analysis [38–41]. In our case the three stationary points $S_i$ are outside the study domain:

$$S_1\begin{pmatrix}1.38\\1.58\\1.33\\-0.46\end{pmatrix} S_2\begin{pmatrix}-0.80\\1.44\\-6.33\\0.77\end{pmatrix} S_3\begin{pmatrix}0.06\\-0.40\\-2.15\\0.46\end{pmatrix}$$

Under these conditions, the canonical analysis consists only in a unique rotation of the co-ordinate system (without translation), which removes the cross-product terms $b_{jk}X_jX_k$ from the mode while keeping the initial origin at the centre point. We shall use $Z_j$ to denote the axes of such rotated system. This will give a canonical model of the form:

$$Y = Y_s + \sum_{j=1}^{j=4} b_j Z_j + + \sum_{j=1}^{j=4} \lambda_j Z_j^2$$

The $\lambda_j$ will describe the curvature of the response while the linear coefficient $b_j$ will describe the slope of the ridge in the corresponding direction. The constant $Y_s$ is the calculated response value at the stationary point. The interpretation is easier by analysing each response along every $Z_j$-axis separately. The canonical analysis is only detailed for the first response i.e. cathodic efficiency. For the two following responses ($Y_2$ and $Y_3$), we only give the final results.

#### 3.2.1. *Study of the cathodic efficiency (response $Y_1$)*

The variable transformations

$$X_1 = -0.15\ Z_1 - 0.04\ Z_2 + 0.45\ Z_3 + 0.88\ Z_4$$
$$X_2 = 0.03\ Z_1 - 0.28\ Z_2 + 0.85\ Z_3 - 0.44\ Z_4$$
$$X_3 = 0.68\ Z_1 + 0.70\ Z_2 + 0.23\ Z_3 + 0.03\ Z_4$$
$$X_4 = 0.72\ Z_1 - 0.65\ Z_2 - 0.15\ Z_3 + 0.17\ Z_4$$

and

$$Z_1 = -0.15\ X_1 + 0.03\ X_2 + 0.68\ X_3 + 0.72\ X_4$$
$$Z_2 = -0.04\ X_1 - 0.28\ X_2 + 0.70\ X_3 - 0.65\ X_4$$
$$Z_3 = 0.45\ X_1 + 0.85\ X_2 + 0.23\ X_3 - 0.15\ X_4$$
$$Z_4 = 0.88\ X_1 - 0.44\ X_2 + 0.03\ X_3 + 0.17\ X_4$$

lead to the following canonical form of the model:

$$\hat{Y}_1 = 22.6 - 13.5\ Z_1 - 14.6\ Z_2 + 7.7\ Z_3 + 7.5\ Z_4 + 16.9Z_1^2 + 10.0Z_2^2 - 1.7\ Z_3^2 - 8.0Z_4^2$$

These data allow us to determine the features of the response surface in each direction of the study domain.

3.2.1.1. *Analysis along the $OZ_1$ direction.* The equation of $\hat{Y}_1$ response is reduced to: $\hat{Y}_1 = 22.6 - 13.5\ Z_1 + 16.9Z_1^2$.

The corresponding curve is represented in Figure 1(1). This curve shows that maximization of $Y_1$ requires low level of $Z_1$. According to the equations of the variable transformations, this can be achieved by choosing low levels (−1) for $X_3$ and $X_4$.

3.2.1.2. *Analysis along the $OZ_2$ direction.* The equation of $\hat{Y}_1$ response is reduced to: $\hat{Y}_1 = 22.6 - 14.6\ Z_2 + 10.0\ Z_2^2$ and represented in Figure 1(2). To increase $Y_1$ it is necessary to progress in the negative direction of $Z_2$-axis. From the equations of the variable transformations, it can be seen that this corresponds to a decrease of $X_3$ and an increase of $X_4$. $Y_1$ is maximum when $X_3 = -1$ and $X_4 = +1$. At this point, we must draw attention to the fact that the choice of the $X_4$ level is opposite to that required increasing $Y_1$ along $OZ_1$-axis.

3.2.1.3. *Analysis along the $OZ_3$ direction.* The equation of $\hat{Y}_1$ response is reduced to: $\hat{Y}_1 = 22.6 + 7.7\ Z_3 - 1.7\ Z_3^2$.

The corresponding curve is represented in Figure 1(3). Any displacement on $Z_3$-axis in the positive direction induces an increase of $Y_1$. Because the $OZ_3$-axis is almost parallel to $OX_2$-axis, $Y_1$ should be optimized by choosing high level (+1) for $X_2$.

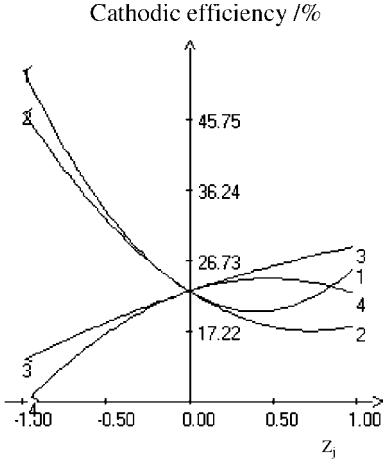


*Fig. 1.* Curvature of $\hat{Y}_1$ response vs. $Z_j$.

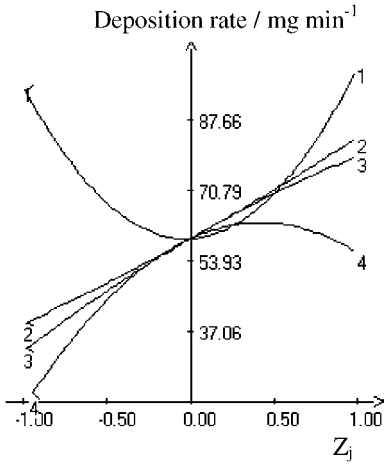


*Fig. 2.* Curvature of $\hat{Y}_2$ response vs. $Z_j$.

3.2.1.4. *Analysis along the $OZ_4$ direction.* The equation of $\hat{Y}_1$ response is reduced to: $\hat{Y}_1 = 22.6 + 7.5\ Z_4 - 8.0\ Z_4^2$ and represented in Figure 1(4). The maximum of $Y_1$ can be obtained for $Z_4$ levels ranging from 0 to 0.4 and therefore for $X_1$ levels varying between 0 and 0.4 ($OZ_4$-axis is almost parallel to $OX_1$-axis).

3.2.2. *Study of the deposition rate (response $Y_2$)*
By the transformation

$$X_1 = -0.06\ Z_1 + 0.39\ Z_2 + 0.34\ Z_3 + 0.85\ Z_4$$
$$X_2 = 0.20\ Z_1 + 0.20\ Z_2 + 0.86\ Z_3 - 0.43\ Z_4$$
$$X_3 = 0.17\ Z_1 + 0.88\ Z_2 - 0.36\ Z_3 - 0.25\ Z_4$$
$$X_4 = 0.96\ Z_1 - 0.18\ Z_2 - 0.09\ Z_3 + 0.18\ Z4$$

and

$$Z_1 = -0.06\ X_1 + 0.20\ X_2 + 0.17\ X_3 + 0.96\ X_4$$
$$Z_2 = 0.39\ X_1 + 0.20\ X_2 + 0.88\ X_3 - 0.18\ X_4$$
$$Z_3 = 0.34\ X_1 + 0.86\ X_2 - 0.36\ X_3 - 0.09\ X_4$$
$$Z_4 = 0.85\ X_1 - 0.43\ X_2 - 0.25\ X_3 + 0.18\ X_4$$

the second order model of $\hat{Y}_2$ becomes:

$$\hat{Y}_1 = 59.2 + 2.3\ Z_1 + 22.4\ Z_2 + 23.4\ Z_3 + 18.5\ Z_4 + 39.0\ Z_1^2 + 2.0\ Z_2^2 - 3.7\ Z_3^2 - 22.1\ Z_4^2$$

The corresponding curves along the four axes are represented in Figure 2. Following the same analysis as above, the deposition rate should be optimized by:
– increasing both $X_2$ (+1) and $X_3$ (+1),
– either increasing or decreasing $X_4$: (+1) or (-1),
– choosing a level for $X_1$ between 0 and 0.4.

3.2.3. *Study of the cobalt content in the Au–Co electrodeposit (response $Y_3$)*
Using the variable transformations:

$$X_1 = 0.84\ Z_1 + 0.53\ Z_2 + 0.01\ Z_3 + 0.15\ Z_4$$
$$X_2 = -0.04\ Z_1 - 0.08\ Z_2 + 0.87\ Z_3 + 0.48\ Z_4$$
$$X_3 = -0.28\ Z_1 + 0.22\ Z_2 - 0.45\ Z_3 + 0.82\ Z_4$$
$$X_4 = -0.47\ Z_1 + 0.82\ Z_2 + 0.20\ Z_3 - 0.27\ Z_4$$

and

$$Z_1 = 0.84\ X_1 - 0.04\ X_2 - 0.28\ X_3 - 0.47\ X_4$$
$$Z_2 = 0.53\ X_1 - 0.08\ X_2 + 0.22\ X_3 + 0.82\ X_4$$
$$Z_3 = 0.01\ X_1 + 0.87\ X_2 - 0.45\ X_3 + 0.20\ X_4$$
$$Z_4 = 0.15\ X_1 + 0.48\ X_2 + 0.82\ X_3 - 0.27\ X_4$$

we obtain the canonical form of $\hat{Y}_3$:

$$\hat{Y}_3 = 1520 - 1379.5\ Z_1 + 71\ Z_2 - 351\ Z_3 - 487\ Z_4 + 1537\ Z_1^2 + 960\ Z_2^2 + 251\ Z_3^2 - 118\ Z_4^2$$

The curvatures of the $\hat{Y}_3$ response along the $OZ_j$ are given in Figure 3. As above, we can deduce that a cobalt content in the Au–Co electrodeposit in the range 2000–3000 ppm can be obtained by fixing:
– $X_1$ in the range (−0.2)–(−0.5),
– $X_3$ at 0.9,
– $X_4$ at −1 or +1.
It is important to point out that varying $X_2$ does not affect $\hat{Y}_3$

3.3. *Optimization*

Table 4 summarizes the experimental conditions, which lead to the optimization of the three separately taken responses.

The overall result of this response analysis suggests that plotting the isoresponse curves as a function of $X_3$ and $X_4$ allows us to find the optimum. The other variables $X_1$ and

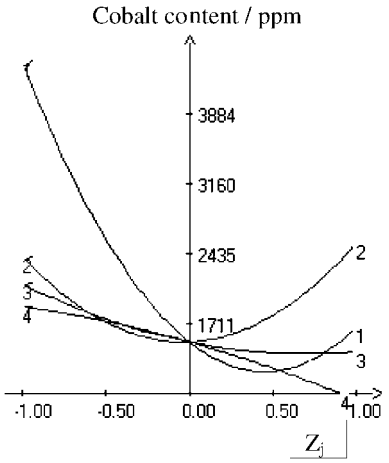


*Fig. 3.* Curvature of $\hat{Y}_3$ response vs. $Z_j$.

*Table 4.* Overall results of the canonical analysis

| | $X_1$ | $X_2$ | $X_3$ | $X_4$ |
|---|---|---|---|---|
| $\hat{Y}_1$ | 0–0.4 | +1 | −1 | ? |
| $\hat{Y}_2$ | 0–0.4 | +1 | +1 | −1 or +1 |
| $\hat{Y}_3$ | (−0.2)–(−0.5) | No effect | 0.9 | −1 or +1 |

$X_2$ should be maintained at the constant levels 0 (to minimize the gold content of the bath) and +1 respectively. Figures 4–6 show the isoresponse contour projection of the three responses. The examination of the isoresponse curves enables to conclude that the best compromise is obtained in a domain around the combination levels of the variables indicated in Table 5. This set of levels gives calculated responses of:

$$\hat{Y}_1 = 43.3\% \quad \hat{Y}_2 = 116.3\,\mathrm{mg\,min^{-1}} \quad \hat{Y}_3 = 2737\,\mathrm{ppm}$$

To validate the calculated optimal conditions, an additional experiment was run with the levels of the optimum. The experimental responses ($\hat{Y}_1 = 43.0\%$, $\hat{Y}_2 = 117.2$ mg˜min$^{-1}$, $\hat{Y}_3 = 2757$ ppm) are in close agreement with the predicted responses.

3.4. *Characteristics of the Au–Co electrodeposit*

The characteristics of the Au–Co electrodeposit corresponding to the 'optimum composition' have been investigated using GDOES and XPS techniques.

Figure 7 shows the GDOES depth profile from the Au–Co electrodeposit with the distribution of C, N, K and Co. Three species (Co, K and N) increase in the outer region of the film, of proportion of the total film thickness (or time abrasion $T$), $T_{\mathrm{outer}}/T_{\mathrm{Au\ deposit}}$ of ≈ 0.15, except for C, revealing a complex variation

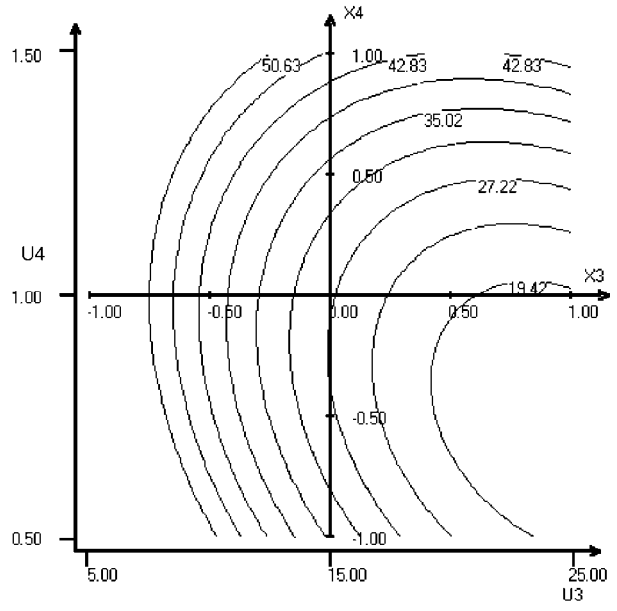


*Fig. 4.* Isocontours of the cathodic efficiency with $X_1$=0 and $X_2$=1.

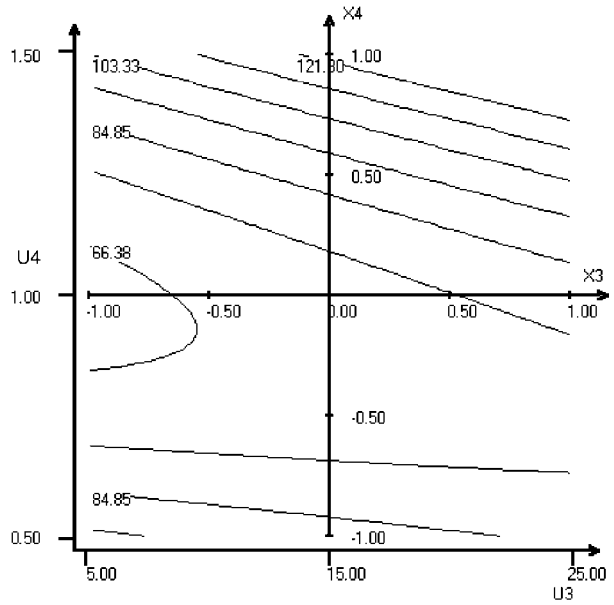


*Fig. 5.* Isocontours of the deposition rate with $X_1$=0 and $X_2$=1.

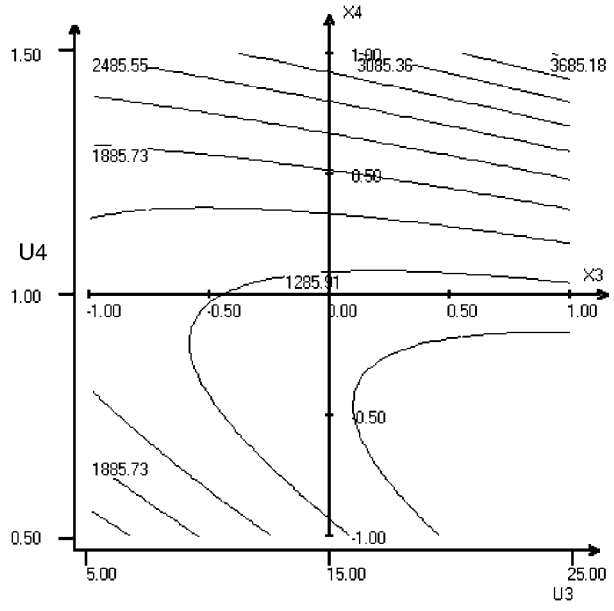


*Fig. 6.* Isocontours of the Co content in the Au–Co deposit with $X_1$=0 and $X_2$=1.

with depth. Beyond this transitional zone, they are uniformly distributed.

XPS analysis shows a surface composed principally of carbon aliphatic form probably due to the adsorption of

*Table 5.* Optimal conditions

| | $X_i$ | $U_i$ |
|---|---|---|
| Gold concentration in the plating bath (g $l^{-1}$) | 0 | 8.5 |
| pH of the plating bath | 1 | 5 |
| Current density (A $dm^{-2}$) | 0 | 15 |
| Cobalt concentration in the plating bath (g $l^{-1}$) | 0.9 | 1.45 |

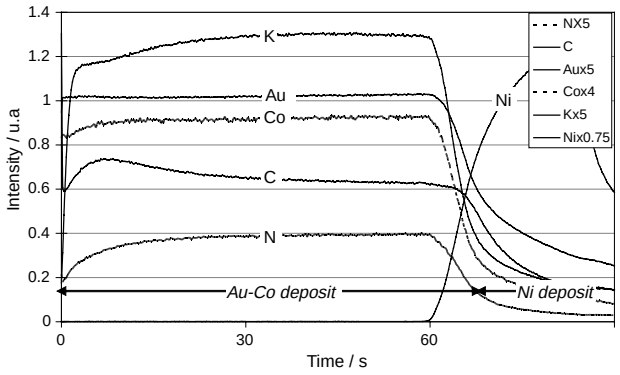


*Fig. 7.* GDOES depth profiles of Au–Co electrodeposit.

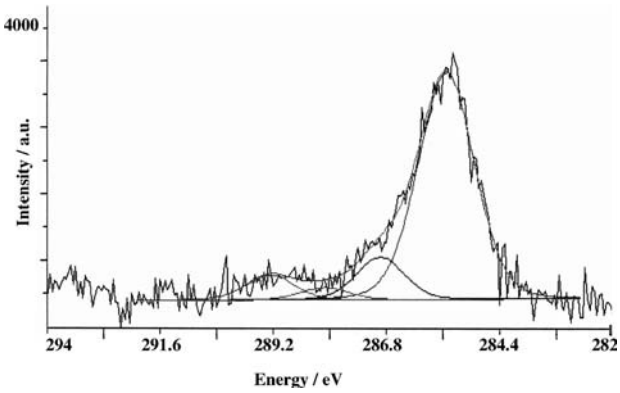


*Fig. 8.* XP spectra of Au–Co electrodeposit. – C 1s.

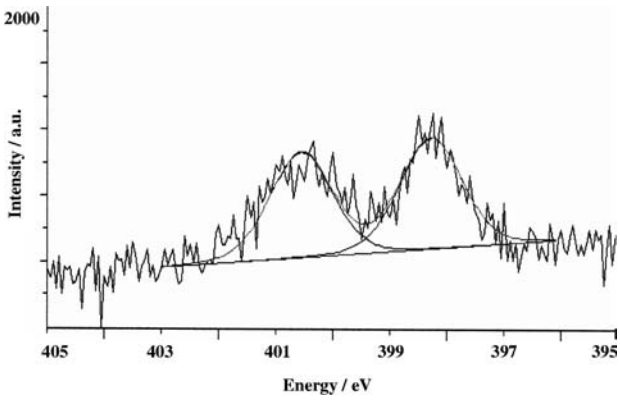


*Fig. 9.* XP spectra of Au–Co electrodeposit. – N 1s.

organic compounds present in the electrolyte (organic acids and salts). Figure 8 reveals four forms of carbon: C—C or C—H at 285 eV [42], C—O or C—N at 286.4 eV [43–45], C=O at 287.6 eV [46] and O—C=O at 288.6 eV [47]. Two forms of nitrogen are also revealed: C≡N at 398 eV [48] and C—N or N—H at 400.5 eV [49] (Figure 9). For cobalt element, two types are detected at 780.7 and 786.9 eV at the extreme surface (Figure 10). The former may correspond to $K_3Co(CN)_6$ [50], while the later cannot be identified because no table reports it. This is neither cobalt metal (778.6 eV) nor

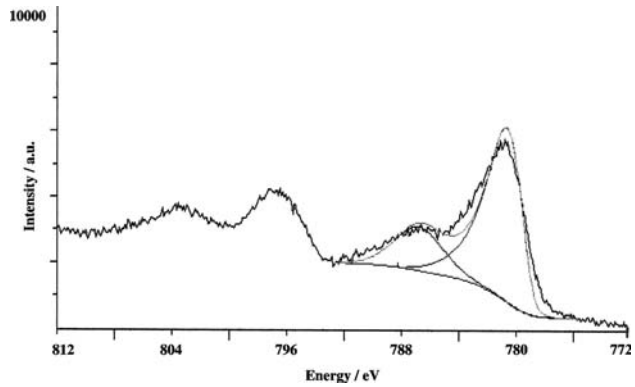


*Fig. 10.* XP spectra of Au–Co electrodeposit. – Co 2p (before abrasion).

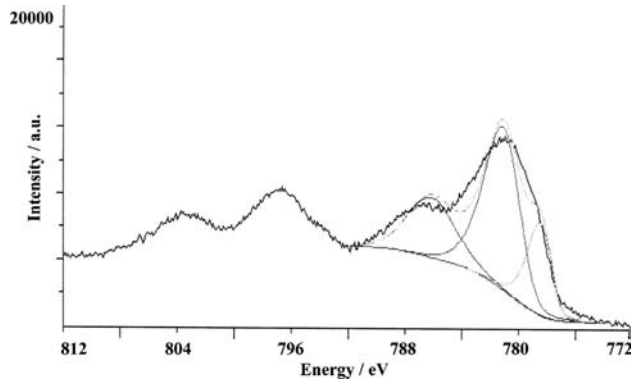


*Fig. 11.* XP spectra of Au–Co electrodeposit. – Co 2p (after abrasion ≈200 Å).

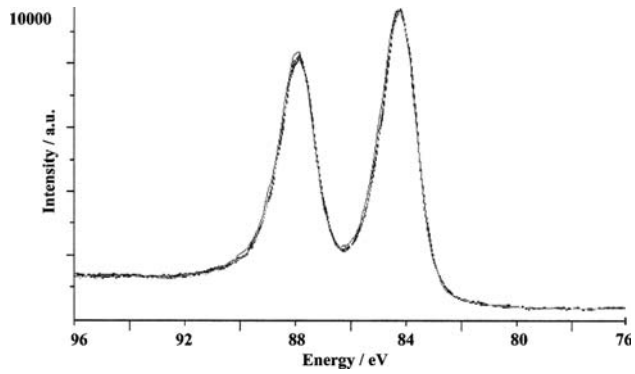


*Fig. 12.* XP spectra of Au–Co electrodeposit. – Au 4f.

*Table 6.* Surface analysis of 2010 electrodeposit by XPS

| | Engold 2010 CHS extreme surface |
|---|---|
| Co (%at) | 4.4 |
| C (%at) | 36 |
| N (%at) | 6.8 |
| O (%at) | 9.4 |
| K (%at) | 0.5 |
| $\frac{[N]}{[C]}$ | 0.19 |

*Table 7.* Proportion of each form of element in Au—Co electrodeposit by XPS

| | Energy /eV | Liaison | Proportion without abrasion /% | Proportion after abrasion (200) /% |
|---|---|---|---|---|
| C | 285.0 | C—C | 77 | |
| | 286.4 | C—O | 12 | |
| | 287.6 | C═O | 4 | |
| | 288.6 | O—C═O | 7 | |
| N | 398.0 | C≡N | 67 | |
| | 400.5 | N orga. | 33 | |
| Co | 778.2 | Co(0) | | 20.3 |
| | 781.9 | $K_3Co(CN)_6$ | 75.6 | 53.6 |
| | 787.4 | | 24.4 | 26.1 |
| Au | 83.8 | Au(0) | 50 | |
| | 88.0 | Au(0) | 50 | |

cobalt oxides ($Co_3O_4$ (780.3 eV) and CoO (780.5 eV)). Nevertheless, after abrasion (200 Å), a third form of cobalt appears at 778.6 eV corresponding to cobalt metal (Figure 11). Gold peaks do not show any chemical shift; this indicates that the gold in the coating is in Au(0) state (Figure 12). The XPS results are summarized in Tables 6 and 7. The aliphatic carbon form may come from buffer and/or organic brightener, which compose the plating electrolyte while the C═O form can be a fragment of a carboxylic acid, such as citric acid. The majority of nitrogen is in the form of C≡N and also in CNO form as demonstrated by the presence of peaks at 286.4 eV of $C_{1s}$ (Figure 8) and at 400.5 eV of $N_{1s}$ (Figure 9). The organic nitrogen may be due to either nitrogen oxide or pyridinic nitrogen of organic brightener.

## 4. Conclusion

Because of the technical and economic importance of electrodeposited cobalt hardened gold, the industrial bath performance and characteristics of the electrodeposit were studied. The achievement of a Doehlert design followed by an optimization allows us to determine the best experimental conditions, which lead to maximization of both cathodic efficiency and deposition rate without a cobalt excess in the Au–Co electrodeposit. An investigation using spectrometric methods (GDOES and XPS) permits us to determine (i) the distribution of C, N, K and Co in the depth of the coating, (ii) the forms of the metallic (Au, Co) and non metallic (C, N) elements at the extreme surface.

## Acknowledgements

Thanks are due to Mrs B. Georges (Sciences et Surface – Lyon France) for the GDOES and XPS measurements and the corresponding calculations and Mrs R.Souissi (E.N.I.S., Tunisie) for her assistance.

## References


1. F.H. Reid and W. Goldie (eds.), *Gold Plating Technology* (Electrochemical Publications, Ayr 1974).
2. M. Antler, *Plating* **60** (1973) 468.
3. Y. Okinaka and M. Hoshino, *Gold Bull.* **31** (1998) 3.
4. V.A. Zabludovskii, A.V. Krapivnoi, V.I. Kaptanovskii and N.A. Kostin, *Elektrokhimiya* **25** (1989) 1258.
5. S.J. Hemsley and R.V. Green, *Trans. Int. Metal Finish.* **69** (1991) 149.
6. R.M. Krishnan, S. Sriveeraraghavan and S.R. Natarajan, *Metal Finish.* **86** (1988) 56.
7. H.U. Galgoon, *Feingerätetechnik* **38** (1989) 353.
8. H. L. Cohen, K.W. West and M. Antler, *J. Electrochem. Soc.* **124** (1977) 342.
9. K. Lin, R. Weil and K. Desai, *J. Electrochem. Soc.* **133** (1986) 690.
10. J.A. Lochet, *Proc. AESF. Annu. Techn. Conf. 77th* Vol. 2. (1990) p.983.
11. S.T. Rao and R. Weil, *Trans. Int. Metal Finish.* **57** (1979) 97.
12. L. Sjögren, B. Asthner, L.G. Liljestrand and L.B. Revay, *Plat. Surf. Finish.* **73** (1986) 70.
13. Y.G. Li, W. Chrzanowski and A. Lasia, *J. Appl. Electrochem.* **26** (1996) 385.
14. Y.G. Li and A. Lasia, *J. Appl. Electrochem.* **26** (1996) 853.
15. Y.G. Li and A. Lasia, *J. Appl. Electrochem.* **27** (1997) 643.
16. A. Blair and D. Becker, *AES Sur/fin'82, Annu. Techn. Conf. 70th* (1983).
17. R.L. Cohen, F.B. Koch, L.N. Schoenberg and K.W. West, *J. Electrochem. Soc.* **126** (1979) 1608.
18. J.H. Thomas III, S.P. Sharma, *J. Electrochem. Soc.* **126** (1979) 445.
19. H. Leidheiser Jr., A. Vertes, M.L. Varsanyi and I. Czako-Nagy, *J. Electrochem. Soc.* **126** (1979) 391.
20. R. De Donker and J. Vanhumbeek, *Trans. Int. Metal. Finish.* **62** (1985) 59.
21. P.Bindra, D. Light, P. Freudenthal and D. Smith, *J. Electrochem. Soc.* **136** (1989) 3616.
22. N.N. Balashova, T.A. Smirnova, N.A. Smagunova and A.K. Yudina, *Zh. Prikl. Khim.* **50** (1977) 2698.
23. H.R. Khan, M. Baugärtner and Ch. J. Raub, In *Proceedings of the Symposium on Electrodeposition Technology: Theory and Practice* (Electrochemical Society, Pennington, NY, 1987) p. 165.
24. T.E. Dinan and H.Y. Cheh, *J. Electrochem. Soc.* **139** (1992) 410.
25. H.A. Reinheimer, *J. Electrochem. Soc.* **121** (1974) 490.
26. F.B. Koch, Y. Okinaka, C. Wolowodiuk and D.R. Blessington, *Plat. Surf. Finishing* **67** (1980) 50.
27. F.B. Koch, Y. Okinaka, C. Wolowodiuk and D.R. Blessington, *Plat. Surf. Finishing* **67** (1980) 43.
28. Y. Okinaka and S. Nakahara, *J. Electrochem. Soc.* **123** (1976) 1284.
29. Ch.J. Raub, A. Knödler and J. Lendvay, *Plat. Surf. Finish.* **63** (1976) 35
30. H.Angerer and N. Ibl, *J. Applied Electrochem.* **9** (1979) 219.
31. A. Knödler, *Metalloberfläche Angwandte Elecktrochemie* **28** (1974) 465.
32. Y. Okinaka, F.B. Koch, C. Wolowodiuk and D.R. Blessington, *J. Electrochem. Soc.* **125** (1978) 1745.
33. R.V. Green and T. Jones, *Trans. Int. Metal Finish.* **75** (1997) 162.
34. T.A. Davies and P. Watson, *Plating* **60** (1973) 1138
35. D.L. Malm and M.J. Vasile, *J. Electrochem. Soc.* **120** (1973) 1484.
36. D. H. Doehlert, *Appl. Statist.* **19** (1970) 231.
37. D. Mathieu, J. Nony and R. Phan Tann-Luu, 'NEMPOD-W software' (LPRAI, Marseille, 2002).
38. D. Mathieu and R. Phan Tann-Luu, In *Plans d'Expériences: Application à l'entreprise* (Technip, Paris, 1995).
39. D. C. Montgomery, In *Design and Analysis of Experiments* (Wiley, New York, 1991).
40. J. Goupy, In *Plans d'Expériences Pour Surfaces de Réponse* (Dunod, Paris, 1999).
41. A.I. Khuri and J.A. Cornell, In *Response Surfaces: Design and Analyses* (M. Dekker, New York, 1996).
42. H.J. Leary, Jr., D.S. Campbell, J.S. Slattery and R.J. Sargent, In ESCA Surface Analysis of Plasma Exposed Silicon Nitride and Photorsist Polymer Films (IBM General Technology Division editor, Essex).
43. R. Erre, R. Benoit, F. Beguin and M. Inagaki, *International Symposium on Carbon* **2** (1990) 6PA 16, 806.
44. P. Sundberg, R. Larsson and B. Folkesson, *Electron Spectrosc. Rel. Phenom.* **46** (1988) 19.
45. V.B. Wiertz and P. Bertrand, In *Identification of the n-containing Functionalities Introduced at the Surface of Ammonia Plasma Treated Carbon Fibres by Combined TOF SIMS and XPS*, Unité de Physico-Chimie et de Physique des Matériaux, Univ. Louvain 1348 Editor, Louvain.
46. N.M.D. Brown, J.A. Hewitt and B.J. Meenan, *Surf. Interface. Analy.* **18** (1992) 187.
47. Q.T. Le, M. Chtaib, J.J. Pireaux and R. Caudano, *Le Vide, les Couches Minces, Supplément* **258** (1991) 86.
48. C.D. Wagner, W.M. Riggs, L.E. Davis and J.F. Moulder, In *Handbook of XPS* (Perking-Elmer Corp., Physical Electronics Division Editor).
49. C. Jones and E. Samman, *Carbon* **28** (1990) 509.
50. K. Merritt, R.S. Wortman, M. Millard and S.A. Brown, *Biomat., Med. Dev., Art. Org.* **11** (1983) 115.